The Time-Domain Theory of Forerunners

Karlsson, Anders; Rikte, Sten

1997

CODEN:LUTEDX/(TEAT-7054)/1-31/(1997)

The Time-Domain Theory of Forerunners

Anders Karlsson and Sten Rikte

Department of Electroscience
Electromagnetic Theory
Lund Institute of Technology
Sweden

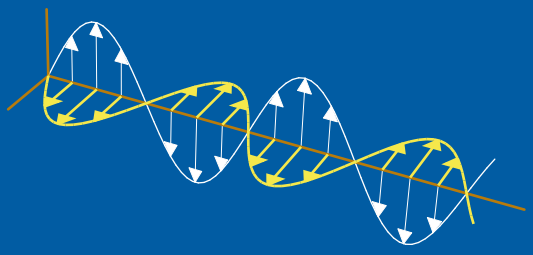

Anders Karlsson and Sten Rikte

Department of Electromagnetic Theory
Lund Institute of Technology
P.O. Box 118
SE-221 00 Lund
Sweden

Editor: Gerhard Kristensson

Abstract

The time-domain theory of forerunners (precursors) in temporally dispersive, nonmagnetic, isotropic materials is developed using the propagator technique. Specifically, the impulse response at a (comparatively) large propagation depth is expanded in two different ways: (a) with respect to the wave-front and (b) with respect to slowly varying field components. A few numerical examples illustrating the theory are given.

1 Introduction

The theory of forerunners or precursors is today a fairly well explored discipline of electromagnetics [1, 2]. The importance of forerunners is due to the fact that transients always arise in electromagnetics (except in strict monochromatic cases) and that all materials exhibit dispersion (to some extent). In other words, many elementary waves are excited and these waves propagate with different phase speed. Absorption in dispersive materials is anomalous resulting in rapidly varying phase speed in certain frequency bands, cf [3].

The first results in the field of forerunners were reported by Arnold Sommerfeld [4] and Léon Brillouin [5] in two consecutive articles under the same title in *Annalen der Physik* in 1914. Sommerfeld and Brillouin used the saddle-point method to analyze pulse propagation in Lorentz (resonance) materials at large propagation depths. In the terminology of the saddle-point method, Sommerfeld's forerunner is due to distant saddle-points (high frequency components), whereas Brillouin's forerunner is due to the saddle-points close to the origin (low frequency components). Sommerfeld's forerunner (the first precursor) is the wave-front behavior of the propagating field. This transient is characterized by high amplitudes and rapid oscillations. Eventually, these oscillations die out, and Brillouin's forerunner (the second precursor) arrives. This anomaly is characterized by a sudden, significant rise in amplitude and a rapid fall in frequency. After the main peak, the amplitude decreases, while the frequency increases. The time when the anomaly occurs is sometimes referred to as the quasilatent time [1]. Sommerfeld showed that the first precursor can be expressed in terms of the Bessel function J_1 with the argument proportional to the square root of the propagation distance and the square root of the wave-front time. Brillouin showed that the second precursor can be expressed in terms of the Airy function Ai, with the argument depending on the propagation distance and the wave-front time in a complicated way. Later, important corrections to the forerunners were obtained using advanced saddle-point methods, see Oughstun and Sherman [2]. In his book, Brillouin foresees a third group of forerunners when more than one resonance frequency are present [1]. Results for such materials are available as well [6]. Recently results on pulse propagation in Debye materials [7, 8] have been published. A physical background of Lorentz and Debye materials, which are the most commonly used models for temporal dispersion, can be found e.g. in [9]– [10].

In the opinion of the authors, Ref. 2 is an exhaustive and trustworthy study

of pulse propagation phenomena in temporally dispersive dielectrics. In the present paper a pure time-domain theory of forerunners in homogeneous, temporally dispersive, nonmagnetic, isotropic materials is developed. It will serve as a complement to the frequency domain theory in Ref. 2. The ambition is to make the theory as general and at the same time as simple and pedagogical as possible.

One-dimensional propagation of pulses in temporally dispersive materials has been treated by many authors. There are, at least, three different time-domain methods that depend on optical wave splitting: the imbedding method [11], the Green functions method [9], and the propagator method [12]. A wave splitting is a change of the dependent variables which simplifies the propagation problem. In this article, a time-domain method based on a dispersive wave splitting is employed. This wave splitting is obtained as a special case of the wave splitting for bi-isotropic media that was originally introduced in [13]. Key concepts are the index of refraction and the wave propagator, which both are temporal integral operators. These operators fully determine the transients of the temporally dispersive medium.

In Section 2, general, normal incidence on a temporally dispersive slab is discussed. A dispersive wave splitting is presented in Section 3 and the corresponding wave propagators are introduced in Section 4. The solution of the propagation problem is given in Section 5. In Section 6, two different expansions of the wave propagator are presented. These expansions correspond to the first precursor and the second precursor. In particular Sommerfeld's forerunner and Brillouin's forerunner are identified. In Section 7, the forerunners for specific material models are discussed. Numerical results are presented in Section 8. In Appendix A, causal fundamental solutions in dispersive media are briefly discussed. Finally, in Appendix B, basic results for some special functions, referred to as hyper-Airy functions, are given. These smooth functions play an important role in the theory of the second forerunner.

2 Basic equations

Throughout this article, Cartesian coordinates $\mathcal{O}(x, y, z)$ are employed. Operators are denoted by calligraphic letters, scalar functions by italic letters, and vectors by italic boldface letters. The radius vector is written $\boldsymbol{r} = \boldsymbol{e}_x x + \boldsymbol{e}_y y + \boldsymbol{e}_z z$, where the basis vectors in the x-direction, y-direction, and z-direction are denoted by $\boldsymbol{e}_x$, $\boldsymbol{e}_y$, and $\boldsymbol{e}_z$, respectively. Time is denoted by t. The electric field intensity and the magnetic field intensity at the space-time point $(\boldsymbol{r}, t)$ are denoted by $\boldsymbol{E}(\boldsymbol{r}, t)$ and $\boldsymbol{H}(\boldsymbol{r}, t)$, respectively. The corresponding flux densities are denoted by $\boldsymbol{D}(\boldsymbol{r}, t)$ and $\boldsymbol{B}(\boldsymbol{r}, t)$. The speed of light in vacuum is denoted by c and the intrinsic impedance of vacuum by η.

The constitutive relations of a linear, homogeneous, temporally dispersive, nonmagnetic, isotropic medium are

$$c\eta \boldsymbol{D}(\boldsymbol{r}, t) = \boldsymbol{E}(\boldsymbol{r}, t) + (\chi * \boldsymbol{E})(\boldsymbol{r}, t), \qquad c\boldsymbol{B}(\boldsymbol{r}, t) = \eta \boldsymbol{H}(\boldsymbol{r}, t), \tag{2.1}$$

where the star indicates temporal convolution:

$$(\chi * \boldsymbol{E})(\boldsymbol{r}, t) = \int_{-\infty}^{t} \chi(t - t')\boldsymbol{E}(\boldsymbol{r}, t')\, dt'.$$

Dispersion is modeled by the electric susceptibility kernel $\chi(t)$, which vanishes for $t < 0$ due to causality and is assumed to be bounded and smooth for $t > 0$. Observe that a temporally dispersive medium with absolutely integrable susceptibility kernel vanishes in the high-frequency limit in electromagnetic sense:

$$\lim_{\omega\to\infty} \int_0^\infty e^{-i\omega t}\chi(t)\, dt = 0 \qquad \text{(the Riemann-Lebesgue lemma)}.$$

The restriction that the medium is nonmagnetic without optical response is not essential.

A general, up-going, linearly polarized plane wave is incident normally on a temporally dispersive slab, $0 < z < d$, see Figure 1. For the sake of simplicity, the medium is assumed to be located in vacuum. The incident plane wave at the front wall, $z = 0$, at time t is given by

$$\boldsymbol{E}^i(t) = \boldsymbol{e}_x E^i(t), \quad \boldsymbol{H}^i(t) = \boldsymbol{e}_y H^i(t), \quad H^i(t) = E^i(t)/\eta.$$

The incident electric field, $E^i(t)$, is assumed to be bounded, smooth, and initially quiescent, i.e., it vanishes for $t < 0$. All electromagnetic fields in the slab are assumed to be initially quiescent.

Transverse electric and magnetic (TEM) solutions of the source-free Maxwell field equations,

$$\nabla \times \boldsymbol{E}(\boldsymbol{r}, t) = -\partial_t \boldsymbol{B}(\boldsymbol{r}, t), \qquad \nabla \times \boldsymbol{H}(\boldsymbol{r}, t) = \partial_t \boldsymbol{D}(\boldsymbol{r}, t),$$

are sought:

$$\boldsymbol{E}(\boldsymbol{r}, t) = \boldsymbol{e}_x E_x(z, t), \qquad \boldsymbol{H}(\boldsymbol{r}, t) = \boldsymbol{e}_y H_y(z, t). \tag{2.2}$$

Elimination of the flux densities yields a first-order system of hyperbolic integro-differential equations in the non-vanishing electric and magnetic field components:

$$c\frac{\partial}{\partial z}\begin{pmatrix} E_x \\ -\eta H_y \end{pmatrix} = \frac{\partial}{\partial t}\left\{\begin{pmatrix} 0 & 1 \\ 1+\chi* & 0 \end{pmatrix}\begin{pmatrix} E_x \\ -\eta H_y \end{pmatrix}\right\}, \qquad 0 < z < d. \tag{2.3}$$

The reflected plane wave at the front wall, $z = 0$, at time t is given by

$$\boldsymbol{E}^r(t) = \boldsymbol{e}_x E^r(t), \quad \boldsymbol{H}^r(t) = \boldsymbol{e}_y H^r(t), \quad H^r(t) = -E^r(t)/\eta.$$

Analogously, the transmitted plane wave at the rear wall, $z = d$, at time t is

$$\boldsymbol{E}^t(t) = \boldsymbol{e}_x E^t(t), \quad \boldsymbol{H}^t(t) = \boldsymbol{e}_y H^t(t), \quad H^t(t) = E^t(t)/\eta.$$

In terms of these scattered waves, the boundary conditions are

$$\begin{aligned} E^i(t) + E^r(t) &= E_x(0, t), \qquad & E^t(t) &= E_x(d, t), \\ H^i(t) + H^r(t) &= H_y(0, t), \qquad & H^t(t) &= H_y(d, t). \end{aligned} \tag{2.4}$$

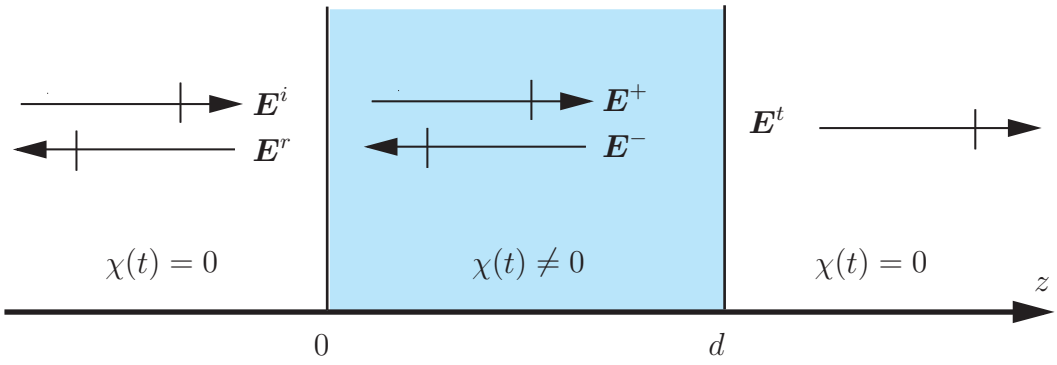

Figure 1: The scattering geometry with the incident, scattered, and internal electric fields indicated.

3 Dispersive wave splitting

One way to deal with propagation problems in temporally dispersive media is to adopt a dispersive wave splitting [13]. New vector field variables are introduced by

$$\begin{pmatrix} E^+ \\ E^- \end{pmatrix} = \mathcal{W} \begin{pmatrix} E_x \\ -\eta H_y \end{pmatrix}, \quad \mathcal{W} = \frac{1}{2} \begin{pmatrix} 1 & -\mathcal{Z} \\ 1 & \mathcal{Z} \end{pmatrix}. \tag{3.1}$$

In terms of the split vector fields, $E^{\pm}(z,t)$, the electric and magnetic fields are

$$\begin{pmatrix} E_x \\ -\eta H_y \end{pmatrix} = \mathcal{W}^{-1} \begin{pmatrix} E^+ \\ E^- \end{pmatrix}, \quad \mathcal{W}^{-1} = \begin{pmatrix} 1 & 1 \\ -\mathcal{N} & \mathcal{N} \end{pmatrix}. \tag{3.2}$$

The temporal integral operators

$$\mathcal{Z} \equiv 1 + Z*, \qquad \mathcal{N} \equiv 1 + N*$$

are the relative intrinsic impedance and the index of refraction (or the relative intrinsic admittance) of the temporally dispersive medium, respectively. The kernels $Z(t)$ and $N(t)$ depend on time only and vanish for $t < 0$. These operators correspond to the complex relative intrinsic impedance and the complex refractive index in the Fourier plane as defined in Ref. 2. By definition,

$$\mathcal{Z}\mathcal{N} = 1 \quad (\mathcal{N} = \mathcal{Z}^{-1}) \quad \text{and} \quad \mathcal{N}^2 = \mathcal{E}_r, \quad \text{where} \quad \mathcal{E}_r \equiv 1 + \chi*$$

is the relative permittivity operator of the medium and 1 the identity operator.

The refractive kernel, $N(t)$, and the impedance kernel, $Z(t)$, satisfy the Volterra integral equations of the second kind

$$\begin{aligned} &2N(t) + (N * N)(t) = \chi(t), \\ &Z(t) + N(t) + (Z * N)(t) = 0. \end{aligned} \tag{3.3}$$

These equations are uniquely solvable in the space of bounded and smooth functions in each bounded time interval, $0 < t < T$, and they are numerically stable as well.

Thus, the construction of $Z(t)$ and $N(t)$ from $\chi(t)$ is a well posed problem. The second Eq. (3.3) can be phrased as: $Z(t)$ is the resolvent kernel of $N(t)$.

Notice that the refractive kernel can be expanded in a power series of temporal convolutions which converges in each bounded time interval, $0 < t < T$:

$$N(t) = \sum_{k=1}^{\infty} \binom{\frac{1}{2}}{k} \left((\chi*)^{k-1}\chi\right)(t).$$

Similarly, the impedance kernel can be expanded in a power series of temporal convolutions:

$$Z(t) = \sum_{k=1}^{\infty} (-1)^k \left((N*)^{k-1}N\right)(t).$$

The dispersive wave splitting (3.1)–(3.2) should be interpreted locally throughout space. Consequently, it reduces to the optical wave splitting outside the slab:

$$E_x = E^+ + E^-, \qquad -\eta H_y = -E^+ + E^-.$$

It is easy to conclude that the split vector fields in the exterior regions are the up-going electric fields and the down-going electric fields, respectively. Fourier transformation of Eq. (3.2) with respect to time shows that this interpretation holds inside the dispersive medium (see also Eq. (3.4) below). At the boundaries, however, the split fields are not well defined. To avoid confusing boundary conditions, the notations $E^{\pm}$ are employed exclusively for the internal fields.

The introduction of the relative intrinsic impedance of the temporally dispersive medium promotes simple, natural definitions of reflection and transmission operators for the electric field at normal incidence at a (single) nondispersive–dispersive interface ($d \to \infty$). In concordance with known results in the Fourier plane, the reflection operator viewed from the nondispersive medium is

$$\mathcal{R} = \big(\eta\mathcal{Z} + \eta 1\big)^{-1}\big(\eta\mathcal{Z} - \eta 1\big) = \big(1 + \mathcal{N}\big)^{-1}\big(1 - \mathcal{N}\big),$$

where the second equality holds for nonmagnetic media only. This temporal integral operator can be written in the form

$$\mathcal{R} \equiv R*,$$

where the kernel $R(t)$ depends on time only and vanishes for $t < 0$. The reflection kernel $R(t)$ satisfies the Volterra integral equations of the second kind,

$$\begin{aligned}
&2R(t) - Z(t) + (Z * R)(t) = 0,\\
&2R(t) + N(t) + (N * R)(t) = 0,\\
&4R(t) + 2(\chi * R)(t) + \chi(t) + (\chi * (R * R))(t) = 0,
\end{aligned}$$

These equations imply that $R(t)$ is bounded, smooth, and continuously dependent on data for $t > 0$. According to the first two equations, $R(t)$ is the resolvent kernel of

$N(t)/2$ and $-R(t)$ is the resolvent kernel of $Z(t)/2$. The third equation is recognized as the imbedding equation for the semi-infinite dispersive medium [11].

Since the reflection operator for the up-going electric field is $\mathcal{R}$, the reflection operator for the down-going electric field is $-\mathcal{R}$. The transmission operator for the up-going electric field is then

$$\mathcal{T} = 1 + \mathcal{R},$$

and the transmission operator for the down-going electric field $1 - \mathcal{R}$. The interpretation of these operators can be affirmed either by Eqs (3.4) and (3.6) below or by temporal Fourier transformation.

Straightforward combination of the Maxwell Eqs (2.3) and the dispersive wave splitting (3.1)–(3.2) shows that the split fields, $E^{\pm}(z,t)$, satisfy first-order dispersive wave equations for up-going and down-going electric fields, respectively:

$$(c\partial_z \pm \partial_t)E^{\pm} = \mp\partial_t N * E^{\pm}, \qquad 0 < z < d. \tag{3.4}$$

Notice that the split fields do not couple. Suppressing the general time-dependence,

$$E^{\pm}(z) := E^{\pm}(z,t), \quad E^i := E^i(t), \quad E^r := E^r(t), \quad E^t := E^t(t), \tag{3.5}$$

the boundary conditions (2.4) at $z = 0$ and at $z = d$ reduce to

$$\begin{pmatrix} E^i \\ E^r \end{pmatrix} = \begin{pmatrix} \mathcal{S} & \mathcal{S}\mathcal{R} \\ \mathcal{S}\mathcal{R} & \mathcal{S} \end{pmatrix} \begin{pmatrix} E^+(0) \\ E^-(0) \end{pmatrix}, \begin{pmatrix} E^t \\ 0 \end{pmatrix} = \begin{pmatrix} \mathcal{S} & \mathcal{S}\mathcal{R} \\ \mathcal{S}\mathcal{R} & \mathcal{S} \end{pmatrix} \begin{pmatrix} E^+(d) \\ E^-(d) \end{pmatrix}, \tag{3.6}$$

respectively, where the temporal integral operator

$$\mathcal{S} \equiv 1 + S*, \qquad \mathcal{S}\mathcal{T} = 1 \quad (\mathcal{S} = \mathcal{T}^{-1})$$

is the inverse (resolvent operator) of the transmission operator $\mathcal{T} \equiv 1 + R*$. The kernel of $\mathcal{S}$ is $S(t) = N(t)/2$.

4 Wave propagators

The solutions of the dynamic equations (3.4) can be written in the form

$$E^{\pm}(z_2, t \pm (z_2 - z_1)/c) = \left[\mathcal{P}\left(\pm\left(z_2 - z_1\right)\right) E^{\pm}(z_1, \cdot)\right](t) \tag{4.1}$$

$(0 < z_1, z_2 < d)$, where the temporal integral operator $\mathcal{P}(z_2 - z_1)$ is referred to as the wave propagator of the temporally dispersive medium and t denotes wave-front time. Due to homogeneity, $\mathcal{P}(z_2 - z_1)$ is invariant under translations in the spatial variable. It is natural, but not necessary, to demand that $z_1 \leq z_2$ $(z_2 \leq z_1)$ for up-going (down-going) fields.

The dynamic equations (3.4) show that the wave propagator satisfies the operator identity

$$\partial_z \mathcal{P}(z) = -\mathcal{K}\mathcal{P}(z), \qquad \mathcal{P}(0) = 1,$$

where the temporal integral operator $\mathcal{K}$ is related to the wave number of the dispersive medium:

$$\mathcal{K} = \frac{1}{c}\partial_t N* = \frac{1}{c}N(0) + K(\cdot)*, \qquad K(t) = \frac{1}{c}N'(t). \tag{4.2}$$

The wave propagator is closely related to the causal fundamental solution of the dispersive wave operator, see Appendix A. In appropriate operator notation,

$$\mathcal{P}(z) = \exp(-z\mathcal{K}). \tag{4.3}$$

Multiplication by the time-shift operator

$$\mathcal{P}_0(z) = \exp\left(-zc^{-1}\partial_t\right) = \delta(\cdot - z/c)*$$

gives a wave propagator, $\mathcal{P}_0(z)\mathcal{P}(z)$, defined in terms of real time. In the frequency plane, this wave propagator corresponds to the propagation factor

$$p(z) = \exp(-ik(\omega)z),$$

where $k(\omega)$ is the complex wave number as a function of angular frequency ω.

Two-fold application of Eq. (4.1) shows that the wave propagator, $\mathcal{P}(z)$, satisfies the relations

$$\begin{aligned} &\mathcal{P}(z_1 + z_2) = \mathcal{P}(z_1)\mathcal{P}(z_2), \\ &\mathcal{P}(0) = 1, \\ &\mathcal{P}^{-1}(z) = \mathcal{P}(-z), \end{aligned} \tag{4.4}$$

where the arguments can be both positive and negative. A positive argument, z, corresponds to propagation of up-going waves or down-going waves in the dispersive medium. A negative argument, $-z$, merely indicates that the inverse (resolvent operator) of the operator $\mathcal{P}(z)$ is referred to. Notice that the rules (4.4) are the requirements for a group; thus, the propagators, $\mathcal{P}(z)$, $-\infty < z < \infty$, form a group. This is of importance in signal restoration since the propagator $\mathcal{P}(-z)$ restores an incident signal $E^+(0,t)$ from a received signal $E^+(z,t)$ by $E^+(0,t-z/c) = [\mathcal{P}(-z)E^+(z,\cdot)](t)$. Multiple propagation through the slab, $0 < z < d$, gives rise to wave propagators with arguments $z > d$.

The wave propagator can be factored as

$$\mathcal{P}(z) = Q(z)\big(1 + P(z;\cdot)*\big), \tag{4.5}$$

where the wave-front propagator, $Q(z)$, is the solution of the ordinary differential equation

$$\partial_z Q(z) = -N(0)Q(z)/c, \qquad Q(0) = 1.$$

This factor determines the attenuation of the wave-front:

$$Q(z) = \exp\left(-\frac{z}{c}N(0)\right).$$

The propagator kernel, $P(z;t)$, satisfies the integro-differential equation

$$\partial_z P(z;t) = -K(t) - \big(P(z;\cdot) * K(\cdot)\big)(t) \qquad P(0;t) = 0, \tag{4.6}$$

which has a unique solution in the space of bounded and smooth functions in each bounded interval, $0 < t < T$, $0 < z < Z$, see Ref. 14. $P(z;t)$ vanishes for $t < 0$ since $K(t)$ vanishes for $t < 0$. By definition, the propagator kernels $P(z;t)$ and $P(-z;t)$ are related to one another by the linear Volterra integral equation of the second kind,

$$P(z;t) + P(-z;t) + \left(P(z;\cdot) * P(-z;\cdot)\right)(t) = 0,$$

for which a unique solution exists.

The propagator kernel can be expanded in a power series of temporal convolutions that converges in each bounded time interval, $0 < t < T$:

$$P(z;t) = \sum_{k=1}^{\infty} \frac{(-z)^k}{k!} \left((K*)^{k-1} K\right)(t). \tag{4.7}$$

In operator notation

$$1 + P(z;\cdot)* = \exp\left(-zK*\right). \tag{4.8}$$

5 Solution of the propagation problem

Suppressing the general time-dependence (3.5), Eqs (4.1) give

$$E^+(z) = \mathcal{P}(z)E^+(0), \qquad E^-(z) = \mathcal{P}(d-z)E^-(d). \tag{5.1}$$

Upon setting $z = d$ in the first equation and $z = 0$ in the second equation, the boundary conditions (3.6) can be exploited, and the four unknown functions $E^{\pm}(0)$, $E^{\pm}(d)$ eliminated. Straightforward calculations show that the solution of the direct scattering problem reads

$$E^t = \mathcal{M}(1-\mathcal{R}^2)\mathcal{P}(d)(\delta_{\frac{d}{c}} * E^i), \qquad E^r = \mathcal{R}E^i - \mathcal{M}(1-\mathcal{R}^2)\mathcal{R}\mathcal{P}(2d)(\delta_{2\frac{d}{c}} * E^i),$$

where the temporal integral operator

$$\mathcal{M} = \left(1 - \mathcal{R}^2\mathcal{P}(2d)\delta_{2\frac{d}{c}} * \right)^{-1}$$

represents multiple propagation through the slab, and the notation

$$(\delta_a * E^i)(t) := E^i(t-a)$$

for time-shift has been employed. For the internal electric fields, the result is

$$E^+(z) = \mathcal{M}\mathcal{T}\mathcal{P}(z)(\delta_{\frac{z}{c}} * E^i), \qquad E^-(z) = -\mathcal{M}\mathcal{T}\mathcal{R}\mathcal{P}(2d-z)(\delta_{\frac{2d-z}{c}} * E^i).$$

Observe that these relations easily can be affirmed heuristically.

If the slab $0 < z < d$ extends to infinity ($d \to +\infty$), the solution of the propagation problem becomes very simple:

$$E^+(z) = \mathcal{T}\mathcal{P}(z)(\delta_{\frac{z}{c}} * E^i) = (1+\mathcal{R})\mathcal{P}(z)(\delta_{\frac{z}{c}} * E^i), \qquad E^-(z) = 0.$$

The total electric and magnetic fields in the medium are then

$$E_x(z) = (1+\mathcal{R})\mathcal{P}(z)(\delta_{\frac{z}{c}} * E^i), \qquad \eta H_y(z) = (1-\mathcal{R})\mathcal{P}(z)(\delta_{\frac{z}{c}} * E^i)$$

and the reflected electric field becomes $E^r = \mathcal{R}E^i$.

A propagation problem closely related to the present one is the internal source problem, where an initially quiescent, transverse current distribution, $\boldsymbol{e}_x J_x(z,t)$, excites the medium, $0 < z < d$. This problem is treated in Appendix A.

6 Expansions of the wave propagator

In this section, the transients (forerunners) of the temporally dispersive medium are investigated. Since the dynamic equations (3.4) have the solutions (5.1), all essential information about the propagating field is contained in the wave propagator, $\mathcal{P}(z)$, which depends on the refractive kernel, $N(t)$, and the propagation depth, z, only. The first precursor and the second precursor can be obtained by expanding the wave propagator in different ways. Recalling the characteristic property of the exponential, this amounts to expanding the refractive kernel appropriately. Sommerfeld's forerunner and Brillouin's forerunner are the leading terms in these expansions.

6.1 The first precursor–Sommerfeld's forerunner

The first precursor is defined as the short-time, or wave-front, behavior of the impulse response

$$[\mathcal{P}(z)\delta](t) = Q(z)\left\{\delta(t) + P(z;t)\right\}, \tag{6.1}$$

where $\delta(t)$ is the Dirac delta pulse. Intentionally, this definition is vague. However, Sommerfeld's forerunner is given a precise meaning below.

In the light of Eqs (4.6)–(4.7), it makes sense to expand the wave-number kernel, $K(t)$, $t > 0$ about $t = 0$. The Maclaurin series of the smooth wave-number kernel is

$$K(t) = H(t)\sum_{j=0}^{k-1}\frac{t^j}{j!}\frac{d^jK}{dt^j}(+0) + H(t)\int_0^t \frac{(t-t')^{k-1}}{(k-1)!}\frac{d^kK}{dt^k}(t')\,dt', \quad k = 1,2,3,\ldots,$$

where $H(t)$ denotes the Heaviside step function. The time-derivatives of the wave-number kernel at the origin, $K^{(k)}(+0) = c^{-1}N^{(k+1)}(+0)$, are obtained from the recurrence relation

$$2N^{(k)}(+0) = \chi^{(k)}(+0) - \sum_{j=0}^{k-1} N^{(j)}(+0)N^{(k-1-j)}(+0),$$

which, in turn, is obtained by differentiating Eq. (3.3) with respect to time. For the first coefficients the result is

$$N(+0) = \frac{1}{2}\chi(+0)$$
$$K(+0) = \frac{1}{2c}\left(\chi'(+0) - \chi^2(+0)/4)\right).$$

Substituting the above expression for $K(t)$ into Eq. (4.8) and using Eq. (4.5) and the fundamental property of the exponential give

$$\mathcal{P}(z) = Q(z)\exp\left(-zK*\right) = Q(z)\left(\prod_{j=0}^{k-1}\mathcal{Q}_j(z)\right)\tilde{\mathcal{Q}}_k(z), \tag{6.2}$$

where the wave-front operators are

$$\mathcal{Q}_j(z) = \exp\left\{-zK^{(j)}(+0)\left(\frac{t^j H(t)}{j!}\right)*\right\}, \qquad j = 0, 1, 2, \ldots, k-1$$

and the remainder is

$$\tilde{\mathcal{Q}}_k(z) = \exp\left\{-\frac{z}{(k-1)!}\left(H(t)\int_0^t (t-t')^{k-1}K^{(k)}(t')\,dt'\right)*\right\}. \tag{6.3}$$

Using the identity $((H*)^n H)(t) = t^n/(n!)H(t)$, the wave-front operators can be written in the form

$$\mathcal{Q}_j(z) = 1 + Q_j(z;\cdot)*, \qquad j = 0, 1, 2, \ldots, k-1,$$

where the power series of the wave-front operators are

$$Q_j(z;t) = H(t)\sum_{i=1}^{\infty}\left(-zK^{(j)}(+0)\right)^i \frac{t^{i(1+j)-1}}{(i(1+j)-1)!i!}.$$

The product (6.2) is an exact expansion of the wave propagator. Approximations to the first precursor are obtained by neglecting the remainder (6.3).

Sommerfeld's forerunner at the propagation depth z is

$$\left[\mathcal{P}_{\mathcal{S}}(z)\delta\right](t) = Q(z)\left\{\delta(t) + P_S(z,t)\right\},$$

where the temporal integral operator is defined by taking the first two factors in expansion (6.2):

$$\mathcal{P}_S(z) = Q(z)\mathcal{Q}_0(z) = Q(z)\big(1 + P_S(z;\cdot)*\big).$$

Since $Q_0(z;t)$ is a Bessel-function expansion, Sommerfeld's forerunner kernel becomes

$$\begin{aligned} P_S(z;t) &= -zK(+0)\left(I_0\left(2\sqrt{-zK(+0)t}\right) - I_2\left(2\sqrt{-zK(+0)t}\right)\right)H(t) = \\ &= -zK(+0)\left(J_0\left(2\sqrt{zK(+0)t}\right) + J_2\left(2\sqrt{zK(+0)t}\right)\right)H(t). \end{aligned} \tag{6.4}$$

The first formula is appropriate for Debye media ($K(+0) < 0$) and the second for Lorentz media ($K(+0) > 0$). This result, which is a generalization of Sommerfeld's result [4] for the single-resonance Lorentz medium, has been obtained before using various methods [15, 16]. Notice that the forerunner in the Lorentz medium is highly oscillating.

6.2 The second precursor–Brillouin's forerunner

The second precursor represents the slowly varying component of the impulse response (6.1). The dominant contribution to this transient is referred to as Brillouin's forerunner. This forerunner will be given a precise meaning below.

An expansion of the wave propagator with respect to slowly varying fields is sought. The general idea is to expand the field in terms of its derivatives and neglect the higher-order terms.

Each smooth field, $E^i(t')$, can be expanded in a Taylor series around the observation time, t:

$$E^i(t') = \left(\sum_{j=0}^{k-1} \frac{(t'-t)^j}{j!} \frac{d^j}{dt^j} E^i(t) \right) + \int_t^{t'} \frac{(t'-t'')^{k-1}}{(k-1)!} \frac{d^k}{dt^k} E^i(t'')\, dt'', \quad k = 1, 2, 3, \ldots .$$

Applying this expansion to the convolution integral $(\chi * E^i)(t)$ gives

$$\left(\chi * E^i\right)(t) = \left(\sum_{j=1}^{k} \chi_j \frac{d^{(j-1)}}{dt^{(j-1)}} E^i(t) \right) + \left(X_k * \frac{d^k}{dt^k} E^i \right)(t), \tag{6.5}$$

where the coefficients

$$\chi_j = \frac{(-1)^{j-1}}{(j-1)!} \int_0^\infty t^{j-1} \chi(t)\, dt \tag{6.6}$$

are proportional to the moments of $\chi(t)$ and the remainder is

$$X_k(t) = \frac{(-1)^k}{(k-1)!} \left(\int_t^\infty (\tau - t)^{k-1} \chi(\tau)\, d\tau \right) H(t).$$

The equality (6.5) can be viewed as an expansion of the operator $\chi*$. Analogously, the operator $N*$ can be expanded as

$$N* = \left(\sum_{j=1}^{k} n_j \frac{d^{(j-1)}}{dt^{(j-1)}} \right) + N_k * \frac{d^k}{dt^k}. \tag{6.7}$$

For media such that X_k and N_k tend to zero as k tends to infinity, one can write

$$\chi* = \sum_{k=0}^{\infty} \chi_{k+1} \frac{d^k}{dt^k} \delta*, \qquad N* = \sum_{k=0}^{\infty} n_{k+1} \frac{d^k}{dt^k} \delta * . \tag{6.8}$$

For instance, these relations hold for the Lorentz model, see Section 7.

Of course, the coefficients χ_k and n_k are closely connected. A relation between these coefficients is obtained by inserting the expansions (6.8) in definition (3.3). The result is

$$\chi_{k+1} = 2n_{k+1} + \sum_{i=0}^{k} n_{k-i+1} n_{i+1}.$$

As a consequence of this recursion formula, it is sufficient to compute the moments (6.6) of the susceptibility kernel. This approach is particularly advantageous

for multiple-resonance media, see Section 7. The coefficients n_k are determined in consecutive order starting with $k = 1$. Explicitly,

$$\begin{aligned} n_1 &= \sqrt{1+\chi_1} - 1, \\ n_2 &= \frac{\chi_2}{2\sqrt{1+\chi_1}}, \\ n_{k+1} &= \frac{\chi_{k+1} - \sum_{i=1}^{k-1} n_{k-i+1} n_{i+1}}{2(1+n_1)}, \qquad k > 1. \end{aligned} \tag{6.9}$$

An expansion of the wave propagator with respect to slowly varying fields can now be obtained. Let $k = k(\chi)$ be less than or equal to the largest integer such that the moment n_k does not violate the signature

$$n_{4k+1} \geq 0, \qquad n_{4k+2} \leq 0, \qquad n_{4k+3} \leq 0, \qquad n_{4k+4} \geq 0. \tag{6.10}$$

Using Eqs (4.2)–(4.3) and expansion (6.7), the wave propagator, $\mathcal{P}(z)$, $z > 0$, can be written as

$$\mathcal{P}(z) = \exp\left\{ -\frac{z}{c}\frac{d}{dt} \sum_{j=1}^{k} n_j \frac{d^{(j-1)}}{dt^{(j-1)}} \right\} \mathcal{P}_{k+1}(z) = \left(\prod_{j=1}^{k} \mathcal{P}_j(z) \right) \mathcal{P}_{k+1}(z), \tag{6.11}$$

where

$$\mathcal{P}_j(z) = \exp\left\{ -\frac{z}{c} n_j \frac{d^j}{dt^j} \right\}, \qquad j = 1, 2, 3, \ldots, k$$

and

$$\mathcal{P}_{k+1}(z) = \exp\left\{ -\frac{z}{c}\frac{d}{dt} N_k * \frac{d^k}{dt^k} \right\}.$$

The propagators $\mathcal{P}_j(z)$ are temporal convolution operators:

$$\mathcal{P}_j(z) = P_j(z;\cdot)*, \quad j = 1, 2, 3, \ldots, k.$$

By definition,

$$P_1(z;t) = \delta\left(t - t_1\right), \quad t_1 = n_1 z/c,$$

where the time-delay t_1 is proportional to the propagation distance z. The kernels $P_j(z;t)$, $j = 2, 3, 4, \ldots, k$ are non-causal. Fourier transformation reveals that

$$P_j(z;t) = \frac{1}{t_j} B_j\left(\frac{t}{t_j}\right), \quad j = 2, 3, 4, \ldots, k,$$

where the scaling times, t_j, are proportional to the jth root of the propagation depth:

$$t_j = \left(\frac{j|n_j|z}{c} \right)^{\frac{1}{j}}, \qquad j = 1, 2, 3, \ldots, k.$$

The properties of the infinitely differentiable, bounded, and integrable hyper-Airy functions $B_j(x) := A_j(-x)$ are discussed in Appendix B. In particular, $A_2(x)$ is

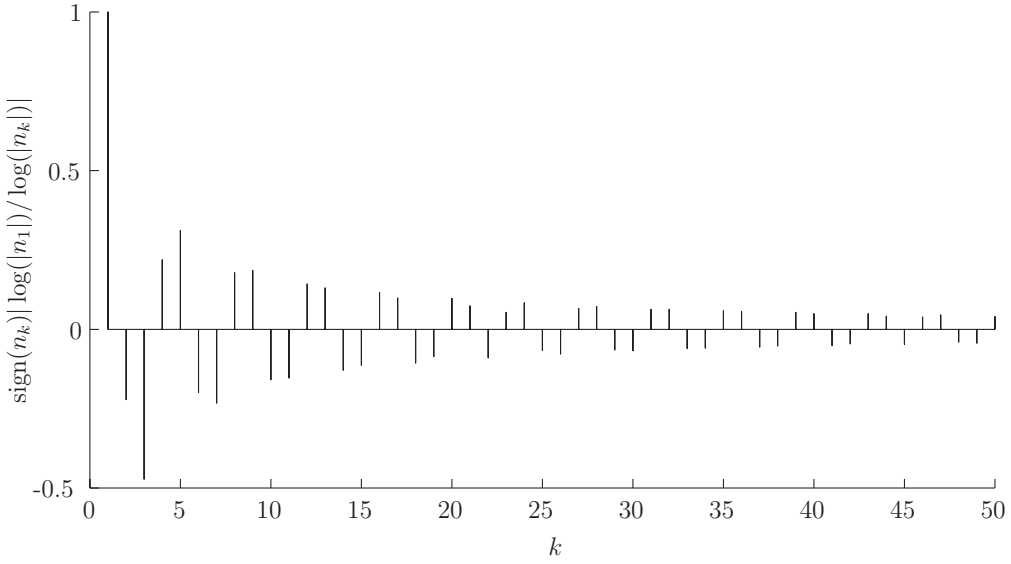

Figure 2: The sign of the coefficients n_k for a single-resonance Lorentz medium with $\omega_p = \sqrt{20} \times 10^{16}\,\mathrm{rad/s}$, $\omega_0 = 4 \times 10^{16}\,\mathrm{rad/s}$ and $\nu = 0.56 \times 10^{16}\,\mathrm{s}^{-1}$. The signature $+--+$ is violated at $k = 23$. This means that the expansion (6.8) has to be truncated at $k < 23$. The coefficients χ_k have the same signs as n_k for the k in this figure. The corresponding propagator kernel is depicted in Figure 3.

a Gaussian function and $A_3(x)$ is the Airy function $Ai(x)$. Observe that for the Lorentz medium, the Airy function comes in backwards in accordance with known results, cf Fig. 3.

As a consequence of Eq. (6.11), the wave propagator, $\mathcal{P}(z)$, can be written as

$$\mathcal{P} = P_1 * P_2 * P_3 * P_4 * ....P_k * \mathcal{P}_{k+1}, \tag{6.12}$$

for some finite integer k. Since the functions $P_j = P_j(z;t)$, $j = 1, 2, 3, \ldots, k$, are smooth, and since the wave propagator can be written in the form (4.5) where the kernel $P(z;t)$ vanishes for $t < 0$ and is bounded and smooth for $t > 0$, the operator $\mathcal{P}_{k+1}(z)$ must produce the highly oscillating field components. In particular, it generates a delta function and Sommerfeld's forerunner kernel. Neglecting the operator $\mathcal{P}_{k+1}(z)$ in the product (6.12) gives a more or less accurate approximation to the slowly varying field components.

The functions $P_k(z;t)$ all satisfy

$$\begin{aligned}
&\int_{-\infty}^{\infty} P_k(z;t)\,dt = 1 \\
&\lim_{z\to 0} P_k(z;t) = \delta(t) \\
&P_k(z_1;t) * P_k(z_2;t) = P_k(z_1+z_2;t)
\end{aligned}$$

It is not possible to have arguments $z < 0$ in $P_k(z;t)$ when $k > 1$ since $P_k(-|z|,t)$ is not a classical function or even a distribution; hence, the inverse to the function

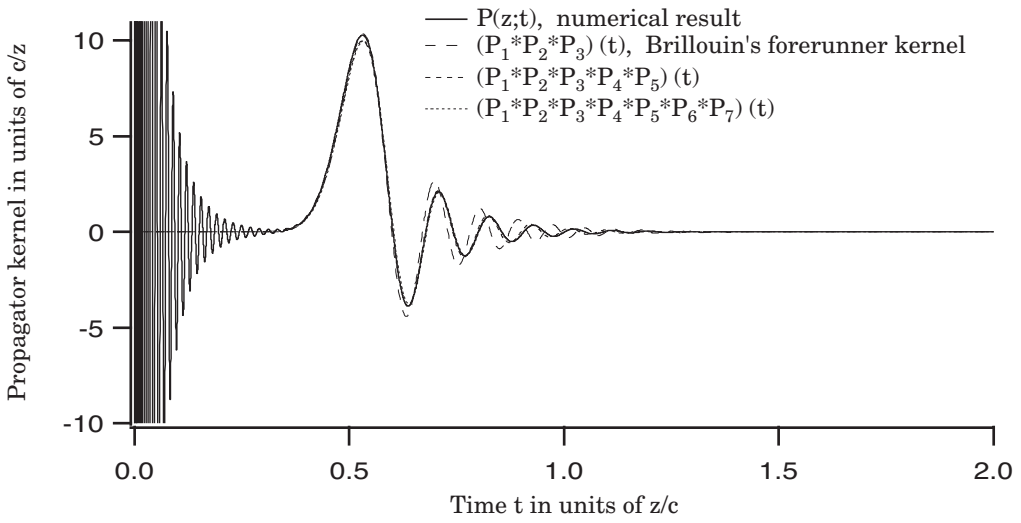

Figure 3: The propagator kernel, $P(z;t)$, for a single-resonance Lorentz medium characterized by Brillouin's parameters ($z = 10^{-6}\,\mathrm{m}$, $\omega_p = \sqrt{20} \times 100/3 \times c/z$, $\omega_0 = 400/3 \times c/z$, $\nu = 56/3 \times c/z$). 32768 data points were used at the equidistant discretization of the time interval $0 < t < 2 \times z/c$. The propagator rule was used once at the computation. Approximations to the second precursor obtained by the time-domain method are shown also. Brillouin's forerunner is an appropriate approximation to the field in the neighborhood of the quasilatent time, $t_1 = 1/2 \times z/c$, only. Higher-order approximations must be used to obtain a good approximation to the "tail" of the second precursor. These approximations practically lie on top of the numerical result.

$P_k(z;t)$ when $k > 1$ does not exist in normal function spaces or in the space of distributions. Thus, for each k, the functions $P_k(z;t)$, $z > 0$ form a semi-group in contrast to the entire propagator, $\mathcal{P}(z)$, $-\infty < z < \infty$, that forms a group. Also if the product in Eq. (6.12) is truncated at some finite $k > 1$ the corresponding propagator does not have an inverse and thus only forms a semi-group.

The theory presented so far holds for the dispersive signature (6.10) only. Examples given below indicate that the above method is well suited for normally absorbing resonance (Lorentz) media for which at least $n_1 > 0$, $n_2 < 0$, $n_3 < 0$, but, perhaps, to restricted to be applied to relaxation (Debye) materials for which $n_1 > 0$, $n_2 < 0$, but $n_3 > 0$. In the following, Brillouin's forerunner is defined for materials for which the refractive coefficients n_1, $n_2 < 0$, and n_3 are finite.

Brillouin's forerunner (kernel), $P_B(z;t)$, is defined by

$$P_B = P_1 * P_2 * P_3, \tag{6.13}$$

where $P_j = P_j(z;t)$, and satisfies the parabolic differential equation

$$-c\partial_z P_B(z;t) = n_1 \partial_t P_B(z;t) + n_2 \partial_t^2 P_B(z;t) + n_3 \partial_t^3 P_B(z;t), \qquad P_B(+0;t) = \delta(t).$$

This definition is essentially the classical, crude approximation to the second precursor in a single-resonance Lorentz material obtained by Brillouin [1]. Temporal

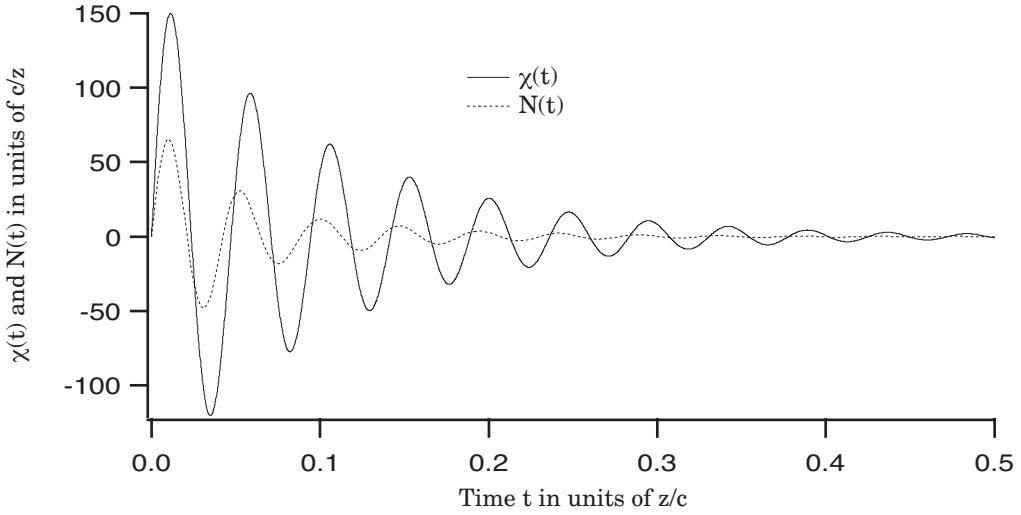

Figure 4: The refractive index, $N(t)$, for the single-resonance Lorentz medium characterized by Brillouin's parameters, cf Figure 3.

Fourier transformation technique gives a closed-form expression for Brillouin's forerunner kernel in terms of the Airy function $Ai(x)$:

$$P_B(z;t) = \exp\left(\frac{n_2^3}{27n_3^2}\frac{z}{c} - \frac{n_2}{3n_3}\left(t - t_1(z)\right)\right)\frac{Ai\left(\mathrm{sign}(n_3)\frac{(t-t_1(z))}{t_3(z)}\right)}{t_3(z)}, \qquad (6.14)$$

where the scaling times are

$$t_1(z) = \left(n_1 - \frac{n_2^2}{3n_3}\right)\frac{z}{c}, \qquad t_3(z) = \left(\frac{3|n_3|z}{c}\right)^{\frac{1}{3}}$$

and the sign function has been introduced: $\mathrm{sign}(n_3) = 1$ for $n_3 > 0$ and $\mathrm{sign}(n_3) = -1$ for $n_3 < 0$. Notice that the quasilatent time $t_1(z)$ has been modified. The result (6.14) can also be verified by straightforward differentiation. Equation (6.14) shows again that Brillouin's forerunner arrives backwards in Lorentz media and forwards in Debye materials.

As has been pointed out before [2], Brillouin's forerunner (6.14) is valid as an approximation to the slowly varying propagating field in a neighborhood of the quasilatent time only. To obtain better approximations to the "tail" of the second precursor, higher-order approximations must be adopted. This can be done either by advanced saddle-point analysis [2] or by using the above convolution technique. In this article, the latter method is employed. In the numerical examples in Section 8, the following expansion is found to be accurate enough: $P_1 * P_2 * P_3 * P_4 * P_5$.

7 The forerunners for specific material models

In this section Sommerfeld's and Brillouin's forerunners are discussed for some specific material models.

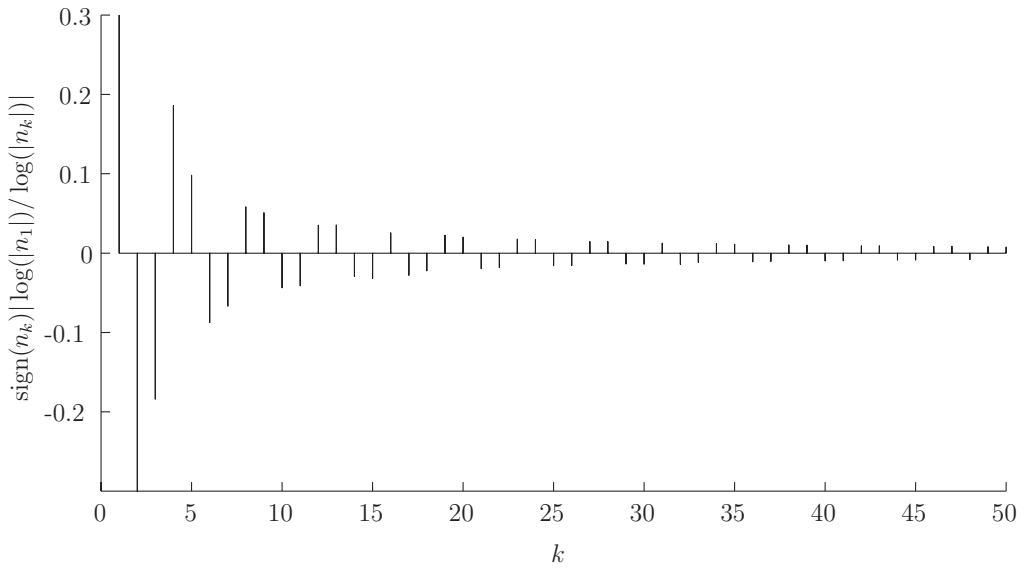

Figure 5: The sign of the coefficients n_k for a double-resonance Lorentz medium with $\omega_{p1} = \sqrt{5} \times 10^{16}\,\mathrm{rad/s}$, $\omega_{01} = 10^{16} \times \mathrm{rad/s}$, $\nu_1 = 0.2 \times 10^{16}\,\mathrm{s}^{-1}$ and $\omega_{p2} = \sqrt{20} \times 10^{16}\,\mathrm{rad/s}$, $\omega_{02} = 10 \times 10^{16}\,\mathrm{rad/s}$, $\nu_2 = 0.56 \times 10^{16}\,\mathrm{s}^{-1}$. The signature $+--+$ is violated at $k = 17$. This means that the expansion (6.8) has to be truncated at $k < 17$. The coefficients χ_k have the same signs as n_k for the k in this figure. The corresponding propagator is depicted in Figure 6.

The susceptibility kernel of the single-resonance Lorentz medium is

$$\chi(t) = \frac{\omega_p^2}{\nu_0} \sin(\nu_0 t) \exp\left(-\frac{\nu}{2}t\right) H(t),$$

where $\nu_0 = \sqrt{\omega_0^2 - \nu^2/4}$. For this particular model, the initial derivatives are

$$\chi^{(k)}(+0) = (-1)^k \frac{\omega_p^2}{2i\nu_0}\left(b^k - \overline{b}^k\right) = (-1)^{k+1} \frac{\omega_p^2 \omega_0^k}{\nu_0} \sin\left(k \arcsin\left(\frac{\nu_0}{\omega_0}\right)\right),$$

where $b = \nu/2 - i\nu_0 = \omega_0 \exp(-i \arcsin(\nu_0/\omega_0))$ and the bar denotes complex conjugate. The initial derivatives satisfy the recurrence formula (cf results for the Chebyshev polynomials)

$$\chi^{(k+2)}(+0) = -\left(\nu\chi^{(k+1)}(+0) + \omega_0^2 \chi^{(k)}(+0)\right).$$

Sommerfeld's forerunner is given by Eq. (6.4) where $N(+0) = 0$ and $K(+0) = \omega_p^2/(2c)$. The relevant properties for the second precursor are

$$X_k(t) = (-1)^k \frac{\omega_p^2}{\omega_0^k \nu_0} \sin\left(\nu_0 t + k \arcsin\left(\frac{\nu_0}{\omega_0}\right)\right) \exp\left(-\frac{\nu}{2}t\right) H(t)$$

and

$$\chi_k = (-1)^{k+1} \frac{\omega_p^2}{\omega_0^k \nu_0} \sin\left(k \arcsin\left(\frac{\nu_0}{\omega_0}\right)\right). \tag{7.1}$$

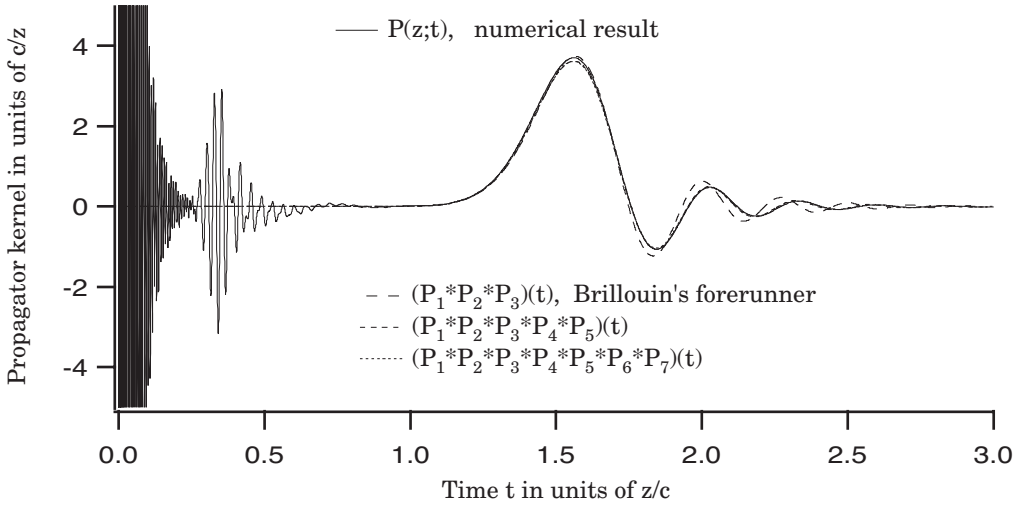

Figure 6: The propagator kernel, $P(z;t)$, for a double-resonance Lorentz medium characterized by the Shen-Oughstun parameters $z = 48\pi \times 10^{-8}\,\mathrm{m}$, $\omega_{p1} = \sqrt{5} \times 16\pi \times c/z$, $\omega_{01} = 16\pi \times c/z$, $\nu_1 = 0.2 \times 16\pi \times c/z$, $\omega_{p2} = \sqrt{20} \times 16\pi \times c/z$, $\omega_{02} = 10 \times 16\pi \times c/z$, $\nu_2 = 0.56 \times 16\pi \times c/z$. 65536 data points were used at the equidistant discretization of the time interval $0 < t < 2 \times z/c$. The propagator rule was used twice. Approximations to the second forerunner are shown as well. As in the single-resonance case, Brillouin's forerunner is an appropriate approximation to the field in the vicinity of the quasilatent time, $t_1 = 3/2 \times z/c$, only. In order to obtain a good approximation to the "tail", higher-order approximations must be used. The higher-order approximations practically lie on top of the numerical result.

From this result, it follows that the susceptibility coefficients χ_k satisfy the recurrence relation

$$\chi_{k+2} = -\frac{1}{\omega_0^2}\left(\chi_k + \nu\chi_{k+1}\right). \tag{7.2}$$

For realistic medium parameters, one has $\chi_1 > 0$, $\chi_2 < 0$, $\chi_3 < 0$, $\chi_4 > 0$:

$$\chi_1 = \frac{\omega_p^2}{\omega_0^2}, \quad \chi_2 = -\frac{\nu\omega_p^2}{\omega_0^4}, \quad \chi_3 = -\frac{\omega_p^2(\omega_0^2 - \nu^2)}{\omega_0^6}, \quad \chi_4 = \frac{\omega_p^2\nu(2\omega_0^2 - \nu^2)}{\omega_0^8}.$$

The first refractive coefficients n_k are

$$n_1 = \sqrt{1 + \frac{\omega_p^2}{\omega_0^2}} - 1 > 0, \qquad n_2 = -\frac{1}{\sqrt{1 + \frac{\omega_p^2}{\omega_0^2}}}\frac{\nu\omega_p^2}{2\omega_0^4} < 0,$$

$$n_3 = -\frac{1}{2\sqrt{1 + \frac{\omega_p^2}{\omega_0^2}}}\left(\frac{\omega_p^2(\omega_0^2 - \nu^2)}{\omega_0^6} + \frac{\nu^2\omega_p^4}{4\omega_0^8}\frac{1}{1 + \frac{\omega_p^2}{\omega_0^2}}\right) < 0.$$

The recurrence relation (7.2) shows that the signature $+--+$ in the susceptibility coefficients, χ_k, is repeated quite a number of times unless the collision frequency ν is

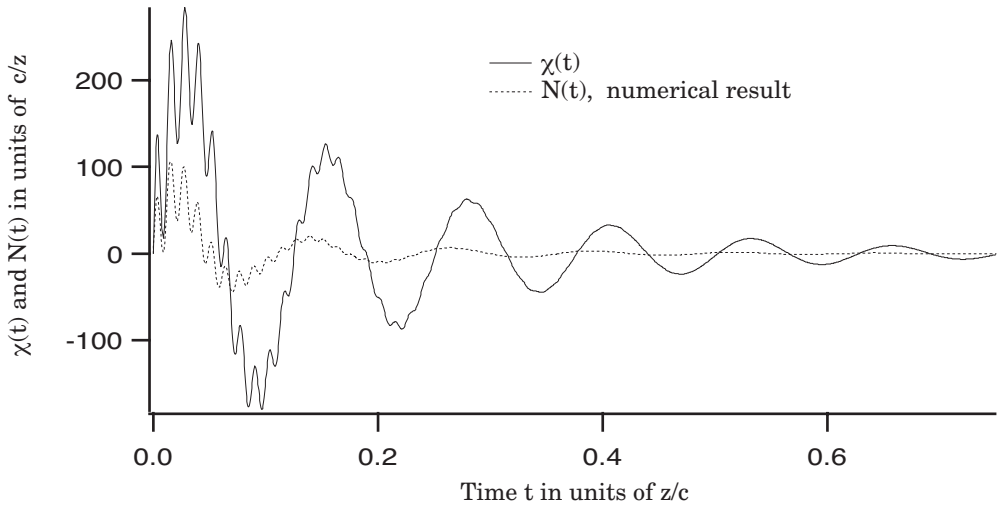

Figure 7: The refractive index, $N(t)$, for the double-resonance Lorentz medium characterized by the Shen-Oughstun parameters, cf Figure 6.

extremely high, cf Figure 2. Experience shows that this is the case for the refractive coefficients, n_k, as well. Brillouin's forerunner kernel is given by Eq. (6.14).

The generalization to a Lorentz medium with M multiple resonant frequencies is straightforward. The susceptibility kernel for such a medium is written as a sum of Lorentz kernels

$$\chi(t) = \sum_{m=1}^{M} \frac{\omega_{p_m}^2}{\nu_{0_m}} \sin(\nu_{0_m} t) \exp\left(-\frac{\nu_m}{2} t\right) H(t).$$

The numbers $N(+0) = 0$ and $K(+0) = \sum_{m=1}^{M} \omega_{p_m}^2/(2c)$ determine Sommerfeld's forerunner. In analogy with Eq. (7.1) the susceptibility coefficients for the second precursor are

$$\chi_k = (-1)^{k+1} \sum_{m=1}^{M} \frac{\omega_{p_m}^2}{\omega_{0_m}^k \nu_{0_m}} \sin\left(k \arcsin\left(\frac{\nu_{0_m}}{\omega_{0_m}}\right)\right).$$

The Debye medium is a very good model for polar liquids in the microwave region. This model reads

$$\chi(t) = \alpha e^{-\beta t} H(t).$$

The relevant properties for Sommerfeld's forerunner are $N(+0) = \alpha/2$ and $K(+0) = -\alpha\beta/(2c) - \alpha^2/(8c)$. The coefficients

$$\chi_k = (-1)^{k-1} \alpha \beta^{-k},$$

determine the second precursor. The three first values of n_k in Eq. (6.9) read

$$n_1 = \sqrt{1 + \frac{\alpha}{\beta}} - 1, \qquad n_2 = -\frac{\alpha}{2\beta^2\sqrt{1 + \alpha/\beta}}, \qquad n_3 = \frac{4\beta\alpha + 3\alpha^3}{8\beta^4(1 + \alpha/\beta)^{3/2}}.$$

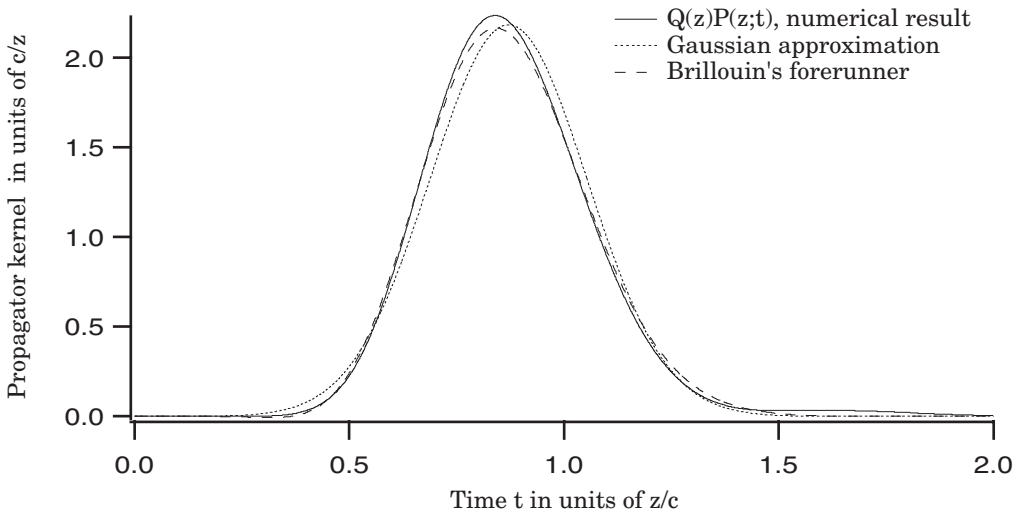

Figure 8: The propagator kernel $Q(z)P(z;t)$ for a Debye half-space characterized by $\alpha = 100 \times c/z$ and $\beta = 40 \times c/z$. 4096 data points were used at the equidistant discretization of the time interval $0 < t < 2 \times z/c$.

The signature $+ - -+$ is broken already at $k = 3$, and then only the two first functions can be used in the expansion (6.12). A better approximation to the propagating field is given by Brillouin's forerunner (6.14).

A model that is used for conducting media is the Drude model. It is obtained from the Lorentz model by letting the resonance frequency ω_0 be zero. The electrons then lose their binding to the atoms and will act as free electrons. Specifically, the susceptibility kernel reads

$$\chi(t) = \frac{\omega_p^2}{\nu} \left(1 - e^{-\nu t}\right) H(t).$$

Sommerfeld's forerunner is then the same as for the Lorentz medium. The susceptibility kernel is not integrable and hence the expansion (6.5) does not exist.

8 Numerical calculations

There is a couple of ways to calculate the propagator kernel, $P(z;t)$, in Eq. (4.5) numerically by time-domain techniques. One way is to solve the integro-differential Eq. (4.6) (by integration along the characteristics, $z =$ constant). This is quite time consuming, since a convolution has to be performed at every step in the spatial variable z. For a fixed propagation depth, z, a more efficient way is to solve the following Volterra integral equation of the second kind:

$$P(z;t) = -\frac{1}{t} \left(F(\cdot) * P(\cdot)\right)(t) - zK(t), \qquad F(t) = ztK(t). \tag{8.1}$$

This equation can be obtained by Laplace transformation of Eq. (4.8) and differentiation with respect to the Laplace transform variable. The integral equation (8.1)

has been used also in Refs 17–18. A straightforward way to solve Eq. (8.1) is to discretize the integral by the trapezoidal rule. The numerical scheme is then very easy to implement. It is also possible to use higher-order integration routines, e.g., the Simpson rule, to get faster convergence. The price to be paid is a more complicated code. A third time-domain method of calculating $P(z;t)$ is to use the series expansion of the exponential in Eq. (4.7). It should be pointed out that the relation

$$P(z_1+z_2;t) = P(z_1;t) + P(z_2;t) + (P(z_1;\cdot) * P(z_2;\cdot))\,(t), \tag{8.2}$$

cf Eq. (4.4), can be utilized in the calculation of $P(z;t)$ in all three cases. In fact, numerical tests indicate that it is necessary to use this rule in order to obtain correct results for (comparatively) large propagation depths.

The asymptotic expressions for $P(z;t)$ are obtained from the analysis in Section 6 and Appendix B. Of the different models presented in Section 7, only the Lorentz models can be expanded in more than two functions in the expansion (8.2). For large z it is enough to use Brillouin's wave propagator (6.14. For smaller z, one has to use more than three functions in the expansion (6.12). The functions P_k with $k > 3$ are, if they exist, obtained from the hyper-Airy functions $A_k(x)$ in Appendix B. For a small argument x, the hyper-Airy function can be obtained numerically by solving the ODE (B.3) with the initial conditions (B.4) and (B.6), or by solving the Volterra Eqs (B.7), or performing the Fourier integral in Eq. (B.1) and Eq. (B.2). Experience indicates that one may switch to the asymptotic expressions presented in Appendix B when x is larger than approximately 5.

In Figure 3 the propagator kernel is shown at depth $z = 10^{-6}$ m for a single-resonance Lorentz half-space characterized by Brillouin's parameters ($z = 10^{-6}$m, $\omega_p = \sqrt{20}\times 100/3\times c/z$, $\omega_0 = 400/3\times c/z$, $\nu = 56/3\times c/z$). The susceptibility kernel, $\chi(t)$, and the refractive kernel, $N(t)$, are depicted in Figure 4. This example was also used in Ref. 19 where the curves were obtained by frequency domain methods. The numerical results shown in Figure 3 were obtained by first solving the integral Eq. (8.1) at $z = 5\times 10^{-7}$ m and then applying the propagator rule (4.4) once. Due to the fast oscillations in the first part of the signal (the first precursor) a large number of data points are needed in such calculations. In this case $32768 = 2^{15}$ data points were used. In Figure 2 the corresponding values of the coefficients n_k are shown. It is then seen that at $k = 23$ the rule $+--+$ is violated. The number of functions in the expansion (6.12) has to be less than 23 but, as seen from Figure 3, already five functions give a very good approximation of the second precursor.

In Figure 6, the propagator kernel, $P(z;t)$, for a double-resonance medium is shown. The parameters and depth z are copied from Ref. 6, where this case was analyzed: $z = 48\pi\times 10^{-8}$ m, $\omega_{p_1} = \sqrt{5}\times 16\pi\times c/z$, $\omega_{0_1} = 16\pi\times c/z$, $\nu_1 = 0.2\times 16\pi\times c/z$, $\omega_{p_2} = \sqrt{20}\times 16\pi\times c/z$, $\omega_{0_2} = 10\times 16\pi\times c/z$, $\nu_2 = 0.56\times 16\pi\times c/z$. The susceptibility kernel, $\chi(t)$, and the refractive kernel, $N(t)$, are depicted in Figure 7. In the calculation of the propagator kernel, the time interval was discretized into $98304 = 3\times 2^{15}$ points and the propagator rule (8.2) was used twice. A small low frequency error can be seen around the scaled time 0.8 where the curve makes a small dip. It is expected that this vanishes if even more points are used. However, the high-frequency signal and the low-frequency signal are very accurate. The main

difference between the propagators in Figures 3 and 6 is the part of the signal that appears between the first and the second precursor in Figure 3. This part is due to the special choice of frequencies in the double-resonance Lorentz model. This contribution cannot be obtained from the expansion (6.12). Another choice of double-resonance parameters, that does not give this kind of response, is analyzed in Ref. 6.

The propagation kernel $Q(z)P(z;t)$ at fixed propagation depth z for a Debye half-space characterized by $\alpha = 100c/z$ and $\beta = 40c/z$ is depicted in Figure 8. Taking the propagation distance to be $z = 1$ m, these parameters correspond to the relaxation time $\tau = 1/\beta = 8.33 \times 10^{-11}$ s and the strength $\alpha = 3 \times 10^{10}$ Hz. The result has been obtained numerically using series expansion of the exponential (4.8). Figure 8 shows that the propagation kernel can be approximated surprisingly well by the normalized Gaussian. Brillouin's forerunner, Eq. (6.14), is an even better approximation.

Conclusion

In this paper the classical problems of the first and second precursors in dispersive media were illuminated from the time-domain. The strategy was to stay in the time-domain as much as possible and only step into the frequency domain to fetch results that are hard to obtain in the time-domain. Many wave-propagation problems can be viewed from both the time-domain and the frequency domain. The present paper manifests that much insight to a wave propagation problem is gained if one has a possibility to view it from both domains.

Acknowledgment

The work reported in this paper is supported by a grant from the Swedish Research Council for Engineering Sciences, and its support is gratefully acknowledged.

Appendix A Causal fundamental solutions

The present article treats external excitation of a homogeneous, temporally dispersive, nonmagnetic, isotropic slab (2.1). In this appendix, the response to an internal current distribution,

$$\boldsymbol{J}(\boldsymbol{r},t) = \boldsymbol{e}_x J_x(z,t), \tag{A.1}$$

is investigated. This source problem is fundamental for one-dimensional wave propagation in temporally dispersive media. Actually, external excitation can be regarded as a special case (with the sources distributed over the boundaries).

The causal fundamental solutions or the retarded Green's functions of the wave operators for up-going waves and down-going waves in an unbounded dispersive medium ($-\infty < z < \infty$) are given in subsection A.1. In subsection A.2, internal excitation of a dispersive slab ($0 < z < d$) is discussed.

A.1 The unbounded dispersive medium

The Maxwell equations are

$$\nabla \times \boldsymbol{E} = -\partial_t \boldsymbol{B}, \qquad \nabla \times \boldsymbol{H} = \boldsymbol{J} + \partial_t \boldsymbol{D},$$

where the current density (A.1) is assumed to bounded and smooth with respect to the time variable and integrable with respect to the spatial variable. A transverse electric and magnetic response of the form (2.2) is sought.

Applying the dispersive wave splitting (3.1)–(3.2) gives the uncoupled, dispersive first-order wave equations

$$\partial_z E^{\pm} = \mp c^{-1} \partial_t \mathcal{N} E^{\pm} \mp \eta \mathcal{Z} J_x/2. \tag{A.2}$$

The split vector fields, $E^{\pm}(z,t)$, can be expressed in terms of the causal fundamental solutions of the dispersive wave operators

$$\pm\partial_z + c^{-1}\partial_t \mathcal{N}.$$

These distributions are denoted by $\mathcal{E}^{\pm}(z;t)$, respectively, and satisfy the dispersive wave equations

$$\left(\pm\partial_z + c^{-1}\partial_t \mathcal{N}\right) \mathcal{E}^{\pm} = \delta(z)\ \delta(t).$$

Under suitable assumptions, Schwartz' kernel theorem [20, pp. 128-129] is applicable, and the solutions of the propagation problems (A.2) can be written in the form

$$E^{\pm}(z,t) = -\frac{1}{2} \int \left(\int \mathcal{E}^{\pm}(z-z';t-t')(\eta \mathcal{Z} J_x)(z',t')\, dt' \right) dz'.$$

It is straightforward to show that the fundamental solutions are

$$\mathcal{E}^{\pm}(z;t) = H\left(\pm z\right) \mathcal{E}(|z|;t),$$

where $H(z)$ is the Heaviside step function and

$$\mathcal{E}(|z|;t) = Q(|z|)\Big(\delta\left(t-|z|/c\right) + P\left(|z|;t-|z|/c\right)\Big),$$

is the retarded fundamental solution of the second-order dispersive wave operator, see Ref. 21. The wave-front propagator, $Q(z)$, and the propagator kernel, $P(z;t)$, were introduced in Section 4.

The special case when the current source is distributed over the plane $z = 0$ is of particular interest. In this case, $J_x(z,t) = j_0(t)\delta(z)$. The up-going and down-going electric fields then satisfy the dispersive first-order wave equations

$$\left(\pm\partial_z + c^{-1}\partial_t(1+N*)\right) E^{\pm}(z,t) = E_0(t)\delta(z),$$

where $E_0 = -\eta(1+Z*)j_0/2$ is the electric field in the plane $z = 0$. Consequently, a current distributed over the plane $z = 0$ induces electric fields given by

$$E^{\pm}(z,t) = \int \mathcal{E}^{\pm}(z,t-t')E_0(t')\, dt',$$

respectively. The relation to the propagator, $\mathcal{P}(z)$, is given by

$$E^{\pm}(z,t+|z|/c) = H(\pm z)\left[\mathcal{P}(|z|)E_0\right](t),$$

that is, $\mathcal{P}(|z|) = \mathcal{E}(|z|,t+|z|/c)* = Q(|z|)(\delta(t)+P(|z|;t))*$.

A.2 Internal excitation of a dispersive slab

The dispersive wave Eqs (A.2) still hold within the slab. Suppressing the general time-dependence (3.5), the boundary conditions (3.6) reduce to

$$E^r = (1-\mathcal{R})\,E^-(0), \qquad E^t = (1-\mathcal{R})\,E^+(d), \tag{A.3}$$

and

$$E^+(0) = -\mathcal{R}E^-(0), \qquad E^-(d) = -\mathcal{R}E^+(d) \tag{A.4}$$

in the absence of external excitation, E^i.

Apart from the given internal current distribution, there is a concentrated source for up-going waves at $z=0$ and a concentrated source for down-going waves at $z=d$. Therefore, the solution of the propagation problem is given by

$$\begin{aligned} E^+(z,t) = &\int \mathcal{E}^+(z,t-t')E^+(0,t')\,dt' \\ &-\frac{1}{2}\int_0^d \left(\int \mathcal{E}^+(z-z';t-t')(\eta\mathcal{Z}J_x)(z',t')\,dt'\right)dz', \qquad 0<z<d \end{aligned}$$

and

$$\begin{aligned} E^-(z,t) = &\int \mathcal{E}^-(z-d,t-t')E^-(d,t')\,dt' \\ &-\frac{1}{2}\int_0^d \left(\int \mathcal{E}^-(z-z';t-t')(\eta\mathcal{Z}J_x)(z',t')\,dt'\right)dz', \qquad 0<z<d, \end{aligned}$$

where the fields $E^+(0,t')$ and $E^-(d,t')$ can be expressed in terms of the fields $E^-(0,t)$ and $E^+(d,t)$ via the conditions (A.4) (notice that these functions satisfy the wave Eqs (A.2) in the interval $0<z<d$, and that trivial results are obtained by letting $z\to 0$ in the first equation and $z\to d$ in the second). Letting $z\to d$ in the first equation and $z\to 0$ in the second gives a system of coupled Volterra integral equations of the second kind in the fields $E^+(d,t)$ and $E^-(0,t)$ only. In terms of the propagator, $\mathcal{P}(z)$, and the multiple propagation operator, $\mathcal{M}$, the solutions are

$$\begin{aligned} E^+(d) = &-\frac{1}{2}\int_0^d \mathcal{M}\mathcal{P}(d-z')\,\eta\mathcal{Z}\left(\delta_{\frac{(d-z')}{c}} * J_x(z')\right)dz' \\ &+\frac{1}{2}\int_0^d \mathcal{M}\mathcal{R}\mathcal{P}(d+z')\,\eta\mathcal{Z}\left(\delta_{\frac{(d+z')}{c}} * J_x(z')\right)dz' \end{aligned}$$

and

$$\begin{aligned} E^-(0) = &\frac{1}{2}\int_0^d \mathcal{M}\mathcal{R}\mathcal{P}(2d-z')\,\eta\mathcal{Z}\left(\delta_{\frac{(2d-z')}{c}} * J_x(z')\right)dz' \\ &-\frac{1}{2}\int_0^d \mathcal{M}\mathcal{P}(z')\,\eta\mathcal{Z}\left(\delta_{\frac{z'}{c}} * J_x(z')\right)dz', \end{aligned}$$

where, for simplicity, the time argument has been dropped. The scattered electric fields, $E^r = E^r(t)$ and $E^t = E^t(t)$, are easily obtained by Eqs (A.3).

Notice that the results above easily can be confirmed heuristically: in each source plane, z', one half of the current density generates an up-going wave whereas the other half generates a down-going wave, and in the observation plane, z, these waves sum up after a number of reflections at the walls.

Appendix B The hyper-Airy functions A_k

The hyper-Airy functions $A_{2k}(x)$, $-\infty < x < +\infty$ are defined as follows:

Definition B.1. *Let k be an arbitrary positive integer. The real function $A_{2k}(x)$ of real argument x is the inverse Fourier transform of the function* $\exp\left(-\xi^{2k}/(2k)\right)$. *The real function $A_{2k+1}(x)$ of real argument x is the inverse Fourier transform of the function* $\exp\left(i\xi^{2k+1}/(2k+1)\right)$.

The hyper-Airy functions $A_{2k}(x)$ of even indices belong to the Schwartz class of rapidly decreasing functions $\mathcal{S}$, that is, the set of all $\phi \in \mathcal{C}^\infty$ such that

$$\sup_x |x^\beta \phi^{(\alpha)}(x)| < \infty$$

for all indices α and β. Thus, in particular, the functions $A_{2k}(x)$ are bounded, infinitely differentiable, and integrable. Moreover, these functions are even functions of x. Explicitly,

$$A_{2k}(x) = \frac{1}{2\pi} \int \exp\left(-\xi^{2k}/(2k) + ix\xi\right) d\xi, \quad -\infty < x < +\infty. \tag{B.1}$$

The hyper-Airy functions $A_{2k+1}(x)$ of odd indices belong to the Schwartz class of tempered distributions $\mathcal{S}'$, that is, the continuous linear forms on $\mathcal{S}$. The generalized functions $A_{2k+1}(x)$ coincide with the bounded, infinitely differentiable, and integrable functions

$$A_{2k+1}(x,\eta) = \frac{1}{2\pi} \int \exp\left(i\zeta^{2k+1}/(2k+1) + ix\zeta\right) d\zeta, \quad -\infty < x < +\infty, \tag{B.2}$$

where the contour of integration is the line $\xi \to \zeta = \xi + i\eta$ and η is an arbitrary positive constant. Since the leading term of the analytic integrand for large $|\xi|$ is $\exp\left(-\xi^{2k}\eta\right)$, the integral (B.2) converges. Moreover, the contour of integration can be displaced in the direction of the imaginary axis, demonstrating that $A_{2k+1}(x,\eta)$ is independent of $\eta > 0$. Since

$$\exp\left(i\zeta^{2k+1}/(2k+1)\right) \to \exp\left(i\xi^{2k+1}/(2k+1)\right) \quad \text{in} \quad \mathcal{S}' \quad \text{as} \quad \eta \to +0,$$

Eq. (B.2) provides integral representations for the hyper-Airy functions $A_{2k+1}(x)$ of odd indices. The leading behaviors of $A_{2k+1}(x)$ as $x \to -\infty$ presented below show that these functions do not belong to the Schwartz class $\mathcal{S}$.

By definition,

$$\int A_k(x)\, dx = 1.$$

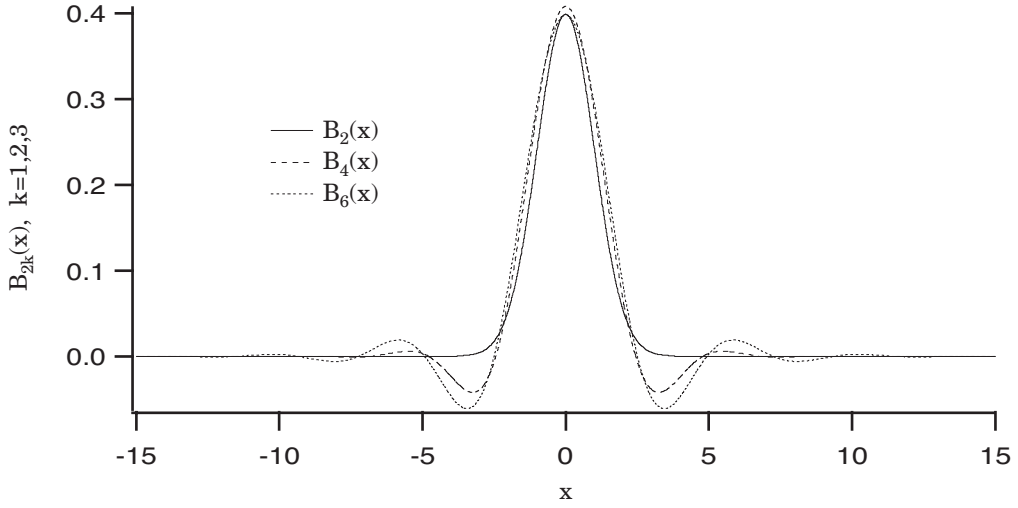

Figure 9: The hyper-Airy functions $B_2(x)$, $B_4(x)$, and $B_6(x)$.

Furthermore, $A_2(x)$ is a Gaussian function and $A_3(x)$ is the Airy function $Ai(x)$:

$$A_2(x) = \frac{1}{\sqrt{2\pi}} \exp\left(-\frac{x^2}{2}\right), \qquad A_3(x) = Ai(x), \qquad -\infty < x < +\infty.$$

Differentiating under the integral sign yields the ordinary differential equations

$$\begin{aligned} A_{2k}^{(2k-1)}(x) &= (-1)^k x A_{2k}(x), \quad -\infty < x < +\infty, \\ A_{2k+1}^{(2k)}(x) &= (-1)^{k+1} x A_{2k+1}(x), \quad -\infty < x < +\infty \end{aligned} \tag{B.3}$$

for the hyper-Airy functions. These equations, which are higher-order generalizations of the Airy equation,

$$Ai''(x) = xAi(x), \quad -\infty < x < +\infty,$$

are sometimes referred to as hyper-Airy equations.

The hyper-Airy equations show that $A_k^{(k-1)}(0) = 0$. More generally, the derivatives of the hyper-Airy functions of even indices at the origin

$$A_{2k}^{(m)}(0) = \frac{1}{2\pi} \int (i\xi)^m \exp\left(-\frac{\xi^{2k}}{2k}\right) d\xi = \frac{i^m}{2\pi} \left(1 + (-1)^m\right) \int_0^\infty t^m \exp\left(-\frac{t^{2k}}{2k}\right) dt$$

can be expressed in terms of the gamma function

$$\Gamma(x) = \int_0^\infty t^{x-1} \exp(-t)\, dt :$$

$$A_{2k}^{(2m)}(0) = \frac{(-1)^m}{\pi} (2k)^{\frac{2m+1}{2k}-1} \Gamma\left(\frac{2m+1}{2k}\right), \qquad A_{2k}^{(2m-1)}(0) = 0. \tag{B.4}$$

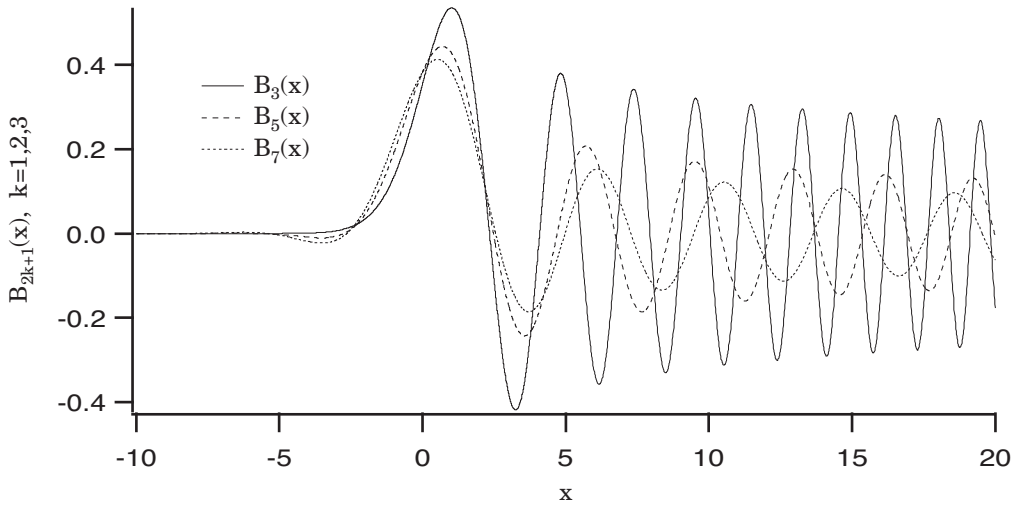

Figure 10: The hyper-Airy functions $B_3(x)$, $B_5(x)$, and $B_7(x)$.

The derivatives of the hyper-Airy functions of odd indices at the origin

$$A_{2k+1}^{(m)}(0) = \frac{1}{2\pi}\int (i\zeta)^m \exp\left(i\zeta^{2k+1}/(2k+1)\right) d\zeta,$$

can be obtained by changing the contour of integration. Integrating along the half-rays

$$\zeta(t) = \mp t \exp\left(\mp \frac{i\pi}{(2k+1)2}\right), \quad t > 0 \tag{B.5}$$

yields the result

$$\frac{i^m}{2\pi}\left(\exp\left(\frac{i(m+1)\pi}{(2k+1)2}\right) + (-1)^m \exp\left(-\frac{i(m+1)\pi}{(2k+1)2}\right)\right)\int_0^\infty t^m \exp\left(-\frac{t^{2k+1}}{2k+1}\right) dt$$

or

$$\begin{aligned} A_{2k+1}^{(2m)}(0) &= \frac{(-1)^m}{\pi}\cos\left(\frac{(2m+1)\pi}{(2k+1)2}\right)(2k+1)^{\frac{2m+1}{2k+1}-1}\Gamma\left(\frac{2m+1}{2k+1}\right), \\ A_{2k+1}^{(2m-1)}(0) &= \frac{(-1)^m}{\pi}\sin\left(\frac{m\pi}{2k+1}\right)(2k+1)^{\frac{2m}{2k+1}-1}\Gamma\left(\frac{2m}{2k+1}\right). \end{aligned} \tag{B.6}$$

Restrictions of the functions $A_k(x)$ to $[0,+\infty)$ and $(-\infty,0]$ can be obtained by solving the hyper-Airy equations subject to the initial values $A_k^{(j)}(0)$, $j = 0,\ldots,k-1$. Good approximations to the hyper-Airy functions can be obtained in the vicinity of the origin using standard ODE-solvers. Convolution equations for the hyper-Airy functions are obtained easily by repeated integration:

$$\begin{aligned} A_{2k}(x) &= \frac{(-1)^k}{(2k-2)!}\int_0^x (x-\xi)^{2k-2}\xi A_{2k}(\xi)\, d\xi + \sum_{m=0}^{2k-2}\frac{x^m}{m!}A_{2k}^{(m)}(0), \\ A_{2k+1}(x) &= \frac{(-1)^{k+1}}{(2k-1)!}\int_0^x (x-\xi)^{2k-1}\xi A_{2k+1}(\xi)\, d\xi + \sum_{m=0}^{2k-1}\frac{x^m}{m!}A_{2k+1}^{(m)}(0). \end{aligned} \tag{B.7}$$

These Volterra equations of the second kind are uniquely solvable in the space of continuous functions in each bounded interval $[0, X]$ or $[-X, 0]$.

The functions $A_k(x)$ can be extended to entire functions in the complex plane. The function $A_k(\omega x)$, where ω is any solution of $\omega^k = 1$, solves the same differential equation as $A_k(x)$. Since the derivative of $A_{2k+1}(\omega x)$ at $x = 0$ is $\omega A'_{2k+1}(0) \neq 0$, and since the second derivative of $A_{2k}(\omega x)$ at $x = 0$ is $\omega^2 A''_{2k}(0) \neq 0$, the functions $A_k(\omega x)$ are all different ($k > 2$). However, the solutions obtained this way are linearly dependent. Specifically, the relationship between these solutions is

$$\sum \omega A_k(\omega x) = 0. \tag{B.8}$$

To prove this fact, compute the derivatives of the left member up to order $k - 1$ at $x = 0$, and use the fact that $\sum \omega^m = 0$ for $1 \leq m \leq k - 1$. The relation (B.8) can be used to obtain asymptotic expansions of $A_k(x)$ on certain half-rays if the corresponding results are known on other half-rays.

Asymptotic expansions for the Airy function $Ai(x)$ are easy to obtain, see, e.g., Hörmander [20]. The leading behavior at large positive arguments x (and the rest of the asymptotic series as well for that matter) is obtained by choosing $\eta = \sqrt{x}$:

$$A_3(x) \sim \frac{x^{-\frac{1}{4}}}{2\sqrt{\pi}} \exp\left(-\frac{2}{3}x^{\frac{3}{2}}\right), \quad x \to +\infty.$$

This result is valid also for complex arguments z, primarily in the opening sector $|\arg z| < \pi/3$, but the expression holds even for $|\arg z| < \pi$. Using this fact and the relation (B.8), one obtains the leading behavior of the Airy function $Ai(x)$ for large negative arguments:

$$A_3(-x) \sim \frac{x^{-\frac{1}{4}}}{\sqrt{\pi}} \cos\left(\frac{2}{3}x^{\frac{3}{2}} - \frac{\pi}{4}\right), \quad x \to +\infty. \tag{B.9}$$

The leading behaviors of the hyper-Airy functions $A_k(x)$, $k > 3$ as $x \to \pm\infty$, which all are oscillating, are now derived. Write

$$A_{2k}(x) = I_{2k}(ix) + I_{2k}(-ix),$$

where the integral

$$I_k(z) = \frac{1}{2\pi} \int_0^\infty \exp\left(-\frac{t^k}{k} + tz\right) dt \tag{B.10}$$

converges for all complex numbers z. For real positive arguments x, the integrand has a movable maximum at $t = x^{1/(k-1)}$. Substituting $s = tx^{-1/(k-1)}$ in the integral (B.10), the maximum is fixed at $s = 1$, and Laplace's method can be used to obtain the leading asymptotic behavior of $I_k(x)$ for large positive arguments:

$$I_k(x) \sim \frac{x^{-\frac{k-2}{2(k-1)}}}{\sqrt{2\pi(k-1)}} \exp\left(\frac{k-1}{k}x^{\frac{k}{k-1}}\right), \quad x \to +\infty, \tag{B.11}$$

see formula (6.4.19c) in Bender and Orzag [22]. The change of variables $s = tx^{-1/(k-1)}$ introduced above shows that this result is valid also for complex arguments z in the opening sector $|\arg z| < \frac{k-1}{k}\frac{\pi}{2}$. Anticipating that the result holds sufficiently far beyond this sector, one obtains the leading behavior of the hyper-Airy functions of even indices:

$$A_{2k}(x) \sim \sqrt{\frac{2}{\pi(2k-1)}}|x|^{-\frac{k-1}{2k-1}} \exp\left(-\frac{2k-1}{2k}\cos\left(\frac{k-1}{2k-1}\pi\right)|x|^{\frac{2k}{2k-1}}\right)$$
$$\times \cos\left(\frac{2k-1}{2k}\sin\left(\frac{k-1}{2k-1}\pi\right)|x|^{\frac{2k}{2k-1}} - \frac{k-1}{2k-1}\frac{\pi}{2}\right), \quad x \to \pm\infty.$$

Observe that the results are not applicable to the Gaussian function — the opening angle is not large enough in this case.

Integrating along the half-rays (B.5), the hyper-Airy functions of odd indices can be expressed in terms of the integral (B.10):

$$A_{2k+1}(x) = \exp\left(-\frac{i\pi}{(2k+1)2}\right) I_{2k+1}\left(-ix\exp\left(-\frac{i\pi}{(2k+1)2}\right)\right)$$
$$+ \exp\left(\frac{i\pi}{(2k+1)2}\right) I_{2k+1}\left(ix\exp\left(\frac{i\pi}{(2k+1)2}\right)\right).$$

Using the leading asymptotic behavior (B.11), one obtains the leading behavior of the hyper-Airy functions of odd indices as $x \to \pm\infty$. The result is

$$A_{2k+1}(x) \sim \frac{x^{-\frac{2k-1}{4k}}}{\sqrt{\pi k}} \exp\left(-\frac{2k}{2k+1}\cos\left(\frac{k-1}{k}\frac{\pi}{2}\right)x^{\frac{2k+1}{2k}}\right)$$
$$\times \cos\left(\frac{2k}{2k+1}\sin\left(\frac{k-1}{k}\frac{\pi}{2}\right)x^{\frac{2k+1}{2k}} - \frac{k-1}{2k}\frac{\pi}{2}\right), \quad x \to +\infty.$$

for large positive arguments and

$$A_{2k+1}(-x) \sim \frac{x^{-\frac{2k-1}{4k}}}{\sqrt{\pi k}} \cos\left(\frac{2k}{2k+1}x^{\frac{2k+1}{2k}} - \frac{\pi}{4}\right), \quad x \to +\infty. \tag{B.12}$$

for large negative arguments. Notice that the result (B.9) for the Airy function $Ai(x)$ for large negative arguments can be obtained using Eq. (B.12). Observe that the results are not applicable to the Airy function $Ai(x)$ for large positive arguments— the opening angle is not large enough.

The results above can be improved retaining more terms in the asymptotic series for $I_k(x)$ as $x \to \infty$. The two first terms are

$$I_k(x) \sim \frac{x^{-\frac{k-2}{2(k-1)}}}{\sqrt{2\pi(k-1)}} \exp\left(\frac{k-1}{k}x^{\frac{k}{k-1}}\right)\left(1 + \frac{(2k-1)(k-2)}{24(k-1)}x^{-\frac{k}{k-1}}\right), \quad x \to +\infty,$$

see formula (6.4.35) in Bender and Orzag [22]. Using this result, the correction term for $A_{2k}(x)$ for large arguments $|x|$ becomes

$$\frac{(4k-1)(k-1)}{12(2k-1)}\sqrt{\frac{2}{\pi(2k-1)}}|x|^{-\frac{3k-1}{2k-1}}\exp\left(-\frac{2k-1}{2k}\cos\left(\frac{k-1}{2k-1}\pi\right)|x|^{\frac{2k}{2k-1}}\right)$$
$$\times\cos\left(\frac{2k-1}{2k}\sin\left(\frac{k-1}{2k-1}\pi\right)|x|^{\frac{2k}{2k-1}}-\frac{3k-1}{2k-1}\frac{\pi}{2}\right).$$

Similarly, the correction term for $A_{2k+1}(x)$ for large positive arguments becomes

$$\frac{(4k+1)(2k-1)}{48k\sqrt{\pi k}}x^{-\frac{6k+1}{4k}}\exp\left(-\frac{2k}{2k+1}\cos\left(\frac{k-1}{k}\frac{\pi}{2}\right)x^{\frac{2k+1}{2k}}\right)$$
$$\times\cos\left(\frac{2k}{2k+1}\sin\left(\frac{k-1}{k}\frac{\pi}{2}\right)x^{\frac{2k+1}{2k}}-\frac{3k+1}{2k}\frac{\pi}{2}\right).$$

Finally, the correction term for $A_{2k+1}(-x)$ for large negative arguments is

$$\frac{(4k+1)(2k-1)}{48k\sqrt{\pi k}}x^{-\frac{6k+1}{4k}}\cos\left(\frac{2k}{2k+1}x^{\frac{2k+1}{2k}}-\frac{3\pi}{4}\right).$$

In summary, the hyper-Airy functions of even indices are even, oscillating functions, which are exponentially attenuated for large arguments. The leading behavior of the hyper-Airy functions of odd indices are oscillating and exponentially attenuated for large positive arguments. The leading behavior of the hyper-Airy functions of odd indices are oscillating but only weakly attenuated for large negative arguments. The frequencies, the phase angles, and attenuating functions can be obtained explicitly in each separate case.

When Brillouin's forerunner is to be discussed, it is more appropriate to use the reversed hyper-Airy functions $B_k(x) := A_k(-x)$ than the hyper-Airy functions themselves. The functions $B_k(x)$, $k = 2, 3, 4, 5, 6, 7$ are plotted in Figure 9 and Figure 10.

References

[1] L. Brillouin. *Wave propagation and group velocity.* Academic Press, New York, 1960.

[2] K. E. Oughstun and G. C. Sherman. *Electromagnetic Pulse Propagation in Causal Dielectrics.* Springer-Verlag, Berlin Heidelberg, 1994.

[3] J. D. Jackson. *Classical Electrodynamics.* John Wiley & Sons, New York, second edition, 1975.

[4] A. Sommerfeld. Über die Fortpflanzung des Lichtes in dispergierenden Medien. *Ann. Phys.*, 44:177–202, 1914.

[5] L. Brillouin. Über die Fortpflanzung des Lichtes in dispergierenden Medien. *Ann. Phys.*, 44:203–240, 1914.

[6] S. Shen and K. E. Oughstun. Dispersive pulse propagation in a double-resonance Lorentz medium. *J. Opt. Soc. Am. B*, 6(5):948–963, 1989.

[7] P. Petropoulos. The wave hierarchy for propagation in relaxing dielectrics. *Wave Motion*, 21(3):253–262, 1995.

[8] T. Roberts and P. Petropoulos. Asymptotics and energy estimates for electromagnetic pulses in dispersive media. *J. Opt. Soc. Am. A*, 13(6):1204–1217, 1996.

[9] G. Kristensson. Direct and inverse scattering problems in dispersive media—Green's functions and invariant imbedding techniques. In R. Kleinman, R. Kress, and E. Martensen, editors, *Direct and Inverse Boundary Value Problems*, Methoden und Verfahren der Mathematischen Physik, Band 37, pages 105–119, Frankfurt am Main, 1991. Peter Lang.

[10] M. Kelbert and I. Sazonov. *Pulses and Other Wave Processes in Fluids*. Kluwer Academic Publishers Group, Dordrecht, 1996.

[11] R. S. Beezley and R. J. Krueger. An electromagnetic inverse problem for dispersive media. *J. Math. Phys.*, 26(2):317–325, 1985.

[12] A. Karlsson. Wave propagators for transient waves in one-dimensional media. *Wave Motion*, 24(1):85–99, 1996.

[13] S. Rikte. The Theory of the Propagation of TEM-Pulses in Dispersive Bi-isotropic Slabs. Technical Report LUTEDX/(TEAT-7040)/1–22/(1995), Lund Institute of Technology, Department of Electromagnetic Theory, P.O. Box 118, S-211 00 Lund, Sweden, 1995.

[14] T. M. Roberts. Causality theorems. In J. P. Corones, G. Kristensson, P. Nelson, and D. L. Seth, editors, *Invariant Imbedding and Inverse Problems*. SIAM, 1992.

[15] A. Karlsson and R. Stewart. Wave propagators for transient waves in periodic media. *J. Opt. Soc. Am. A*, 12(7):1513–1521, 1995.

[16] S. Rikte. Sommerfeld's forerunner in stratified isotropic and bi-isotropic media. Technical Report LUTEDX/(TEAT-7036)/1–26/(1994), Lund Institute of Technology, Department of Electromagnetic Theory, P.O. Box 118, S-211 00 Lund, Sweden, 1994.

[17] A. Karlsson. Inverse scattering for viscoelastic media using transmission data. *Inverse Problems*, 3:691–709, 1987.

[18] P. Fuks, A. Karlsson, and G. Larson. Direct and inverse scattering for dispersive media. *Inverse Problems*, 10(3):555–571, 1994.

[19] K. E. Oughstun and G. C. Sherman. Propagation of electromagnetic pulses in a linear dispersive medium with absorption (the Lorentz medium). *J. Opt. Soc. Am. B*, 5(4):817–849, 1988.

[20] L. Hörmander. *The Analysis of Linear Partial Differential Operators I.* Grundlehren der matematischen Wissenshaften 256. Springer-Verlag, Berlin Heidelberg, 1983.

[21] S. Rikte. One-dimensional pulse propagation in temporally dispersive media — exact solutions versus numerical results. Technical Report LUTEDX/(TEAT-7053)/1–35/(1997), Lund Institute of Technology, Department of Electromagnetic Theory, P.O. Box 118, S-211 00 Lund, Sweden, 1996.

[22] C. M. Bender and S. A. Orszag. *Advanced Mathematical Methods for Scientists and Engineers.* McGraw-Hill, New York, 1978.